Effect of temperature on the growth of TiN thin films by oblique angle sputter-deposition: A three-dimensional atomistic computational study

Rubenson Mareus, Cédric Mastail, Florin Nita, Anny Michel, Grégory Abadias

Effect of temperature on the growth of TiN thin films by oblique angle sputter-deposition: a three-dimensional atomistic computational study

Rubenson Mareus[1,2], Cédric Mastail[1], Florin Nita[1,3], Anny Michel[1], Grégory Abadias[1]

[1]Institut Pprime, UPR 3346, Département Physique et Mécanique des Matériaux, CNRS-Université de Poitiers-ENSMA, 11 Bd Marie et Pierre Curie – TSA 41123, 86073 Poitiers Cedex 9, France

[2]Département Physique, Université d'Etat d'Haïti-Ecole Normale Supérieure, Laboratoire des Sciences pour l'Environnement et l'Energie (LS2E), HT6115 Canapé-Vert, Port-au-Prince, Haïti

[3]National Institute for Research and Development in Microtechnologies - IMT Bucharest, 126A Erou Iancu Nicolae Street, 077190, Voluntari, Ilfov, Romania

Abstract

Kinetic Monte Carlo (kMC) atomistic computations using MODENA code were employed to simulate the growth of columnar TiN thin films under oblique angle deposition geometry. The influence of substrate temperature (300, 400 and 500 K) on the morphology (column tilt angle, average layer density, compactness, surface roughness) of the layers was studied by varying the inclination angle α of the substrate from 5° to 85° with respect to the centerline of the source. Two types of simulations were considered in this work: the first one assumes a collimated flux (CF) of incident particles and the second one grasps the angular distribution of sputtered Ti particles to closely mimic the magnetron sputtering (MS) conditions. The formation of separated columns with high aspect ratio, and tilted in the direction of the incident particles flux, is observed for $\alpha \geq 35°$ for the two types of particle flux. The column width and tilt angle, the average layer density and the compactness of the TiN films are found to increase with increasing substrate temperature, due to enhanced surface diffusion. The column tilt angle β increases from 3° to 60° with increasing α for the CF case, while it saturates to approx. 35° when the MS distribution is considered. The relationship between β and α, and their temperature dependence, are discussed and compared to experimental results obtained on sputter-deposited TiN films, as well as with other results and models reported in the literature. The code also reproduces morphological features common to most films

produced at glancing angles, such as column broadening with increasing thickness and their anisotropic aggregation (bundling association) in the transverse direction.

Keywords: TiN; tilted columns; Monte Carlo simulations; angular distribution; GLAD; magnetron sputtering

1. Introduction

Oblique angle deposition (OAD) is a proven and easy-to-handle physical vapor deposition technique that adapts film architectures and controls film properties such as microstructure, texture, porosity, surface area and anisotropy within the film plane [1–3]. A large palette of thin film morphologies can be achieved by appropriate control of the incidence angle θ of the particle flux with respect to the substrate normal or by monitoring dynamically the substrate motion: films produced by OAD can be developed as inclined columns [4,5], zigzag columns [6,7], nano-spirals [8], nanorods/nanowires [9–11] or nanotrees [12,13]. If the flux impinging on the substrate is highly directional, as involved in thermal evaporation, the formation of isolated columns with high aspect ratios and inclined towards the incoming vapor flux is typically observed at large θ angles (> 60°) and without substrate rotation. The resulting film porosity may achieved values up to 80% [14], which has significance for a number of applications [3]. Nanostructured thin films produced by OAD technology find important applications in various fields, such as gas detection [15,16], optical and photonic devices [4,17–20], photovoltaic and fuel cell components [21–23], supercapacitors [24,25], as well as surfaces with controlled wettability [26] and biocompatibility [27].

The development of such inclined columnar structures is primarily governed by self-shadowing from neighboring columns under conditions of low adatom mobility [28]. Due to

the oblique incidence geometry, the growing nuclei cast a shadowed region over which the other particles cannot condense, unless significant surface diffusion processes can be thermally activated [29]. Besides the geometrical configuration of the substrate and particle source, the morphology of OAD films depends on a number of deposition parameters, which include deposition rate, substrate temperature, energy and angular distribution of the impinging flux.

The design and engineering of materials and devices with specific morphological features and functionalities requires a thorough understanding on how these parameters affect the growth process. For example, the column tilt angle β (with respect to the substrate normal) varies with the angle of incidence θ of the deposited atoms. Early works have tried to establish some universal laws founded on empirical observations [30] or models [31,32]. However, recent experimental works and numerical simulations have shown that the $\beta(\theta)$ relationship is material and growth conditions dependent [33–37]. In particular, the influence of substrate temperature on the degree of column tilt is far to be fully understood, because literature reports appear contradictory either from experimental observations [29,37–41] or based on computer simulations/continuum models [28,31,42,43]. This is because directional (conservation of parallel momentum) and random surface diffusion have antagonist effects on column inclination, as pointed out originally by Hara *et al*. [44]. Later, Abelman and Lodder [29] conclusively confirmed the importance of these two factors, besides mentioning that surface contamination may also play a role.

In an effort to contribute to addressing the issue on how surface diffusion affects self-shadowing and column inclination, we investigate in the present work the temperature dependence of the morphology of TiN thin films under OAD geometry using a computational approach. Our three-dimensional (3D) atomistic simulations are based on a kinetic Monte Carlo (kMC) algorithm that incorporates both ballistic deposition and surface diffusion

processes. This methodology was successfully employed to predict the growth and morphological features of TiN thin films deposited at normal incidence [45] or by OAD at room temperature and varying working pressure [46]. Here, we apply the developed MODENA simulator to systematically study the influence of substrate temperature (in the 300-500 K range) on the development of TiN columnar microstructures obtained at varying substrate inclination angles ($5° \leq \alpha \leq 85°$). Different angular distributions of the impinging particle flux are considered, to explore different deposition process specificities. A detailed analysis of the computed microstructures will be presented along this work and the $\beta(\alpha)$ profiles obtained at different temperatures will be discussed and compared to experimental β values of TiN OAD films produced by reactive magnetron sputtering (MS). The choice of TiN system is motivated by the fact that transition metal nitride (TMN) thin films and nanostructures produced by OAD hold great promise in the realm of refractory plasmonics and energy storage applications [11,24,47–52]. However, experimental studies on the microstructural development of TMN thin films by OAD remain relatively scarce [6,53–56].

2. Methodology

All atomistic simulations were performed using a kMC algorithm to study the growth morphology of TiN thin films deposited on substrates making different inclination angles α= 5, 35, 65, 75 and 85° with respect to the centerline of the particle source (Ti target), see Figure 1. The kMC model is based on a 3D rigid lattice of cubic symmetry (Na-Cl type), and considers deposition and diffusion events for both Ti and N species, as depicted in Figure 1. The substrate surface normal z is oriented along the [001] direction of the TiN crystal lattice. Particles are randomly generated at (x,y) positions above the simulation box and being assigned initial trajectories with a given angular distribution. The energy of the incoming particle is implicitly taken into account by varying the radial distance r_0 measured between

the particle trajectory and a possible deposition site belonging to a neighborhood surface (the interaction parameter – see below).

Two different sets of simulations were performed depending on the distribution type of the particle flux. The first one involves a collimated flux (CF), in which it is assumed that the flux of incident particles approaches the surface of the substrate along a rectilinear trajectory, i.e., the particles emitted from the target are transported in the gas phase with no deviations, and therefore the incident angle θ of any arriving particle is equal to the geometrical angle α (with a Gaussian dispersion $\Delta\alpha = 0.01°$). The CF condition is representative of growth by thermal evaporation but can also mimic depositions with the use of a collimator to take advantage of exacerbated shadowing effect at glancing angles (α~80-90°). Considering a dispersion $\Delta\alpha$ is a necessary condition to obtain 3D nanocolumns, as demonstrated by Alvarez *et al*. [57]. The second set of simulations is representative of MS conditions and considers interaction of the particle flux with gas atoms before reaching the substrate. Due to scattering of particles in the gas phase (mainly with Ar atoms from the plasma), the angular distribution can be relatively broad so that the incident angle θ of particles reaching the substrate may notably differ from α. In the present work, we consider the angular distribution of Ti particles at a working pressure of 0.3 Pa, which corresponds to the working pressure used for the experiments. To avoid adding complexity to the system, the same distributions were also assumed for N particles. These distributions are shown in Figure 2 for the different substrate inclination angles α investigated. They are computed using the SIMTRA code [58], which requires as input files the kinetic energy and angular distribution of the particles leaving the target, which are here obtained using the SRIM code [59]. SRIM and SIMTRA are both Monte Carlo simulations. The advantage of the SIMTRA code is that the specific geometric dimensions of the deposition chamber are taken into account, allowing for a direct

comparison with the experiments. The overall multi-approach Monte-Carlo-based methodology can be visualized in Figure 1 for the case of MS conditions.

The MODENA code (MOdelling DEposition of Nitride films and their Alloys) is an undistributed laboratory software that simulates the growth in 3D of TMN thin films with a cubic structure. This simulator was specifically developed to study the TiN system. It uses the superposition of two fcc sub-lattices (metal and nitrogen) to model the cubic rock-salt structure of TiN. The lattice parameter was fixed to the TiN bulk value, i.e., a_0 = 0.424 nm. A complete description of the kMC model can be found elsewhere [45]. In this work, we apply our model to predict the growth morphologies of TiN thin films deposited at different oblique angles and at varying substrate temperatures. Both deposition and diffusion events are considered in the model. A bond-counting model (model #2 in Ref. [45]) is assumed for the diffusion events, considering nearest- and next-nearest neighbors of a diffusing particle (Ti or N single atom). Surface diffusion events were observed at 400 K and 500 K, but not at 300 K taking into account the relatively large activation barrier E_0 of 1.0 eV chosen for both N and Ti diffusing species [45]. Note that the same E_0 value was considered independently of the local orientation of the surface and nature of diffusing particles. The value of 1.0 eV is taken as the average of available computed values from the literature for (001), (110) and (111) surfaces [60–62]. For deposition events, the interaction parameter between the incoming particle and the 3D surface was fixed at a distance $r_0 = \frac{\sqrt{2}}{2}a_0$, where r_0 is the radius of the cylinder drawn along the particle trajectory and inside which the possible available deposition sites are selected (see Figure 1). This approach allows mimicking incoming particles trapping due to short-range interactions with the film surface, similarly to the procedure employed by Alvarez *et al*. [63]. The deposition and diffusion events occur on stable sites defined as sites obeying a well-defined surface contact rule, i.e. having a minimum number of nearest (N_{nn}) and next-nearest (N_{nnn}) neighbors. Here, the surface contact rule is fulfilled when $N_{nn} \geq 1$ and

$N_{nnn} \geq 3$. This set of parameters allows reproducing more realistic film properties, as shown in our previous work [45]. All simulations are performed in a box with dimensions of 200×200×100 unit cells, leading to a simulated volume of ~3.8 $10^{-5}\mu m^3$. This corresponds to approximately 4×10^6 atoms for the densest films. The deposition rate was fixed to one monolayer (ML) per second (0.212 nm/s) for all simulations.

The simulated TiN growth morphologies were visualized using OVITO [64] and AtomEye [65] software and several morphological features were analyzed. From cross-sectional views, the column tilt angle β was determined as the average of the column inclination angle (with respect to the substrate normal) from a sampling of 10 columns, and then the error bar taken as the standard deviation. The analysis was performed in the middle part of the simulated TiN cross-section images to avoid effects from the substrate interface as well as the influence of column bending at larger film thickness, as also observed experimentally. The film compactness C was quantified as the ratio between the number of particles having six nearest-neighbor occupied sites to the total number of deposited particles. We also extracted the average layer density, ρ(z), defined as the ratio of all occupied sites in the (x,y) plane at a given z coordinate to the total number of sites in this plane. Both these quantities give an estimation on the film porosity.

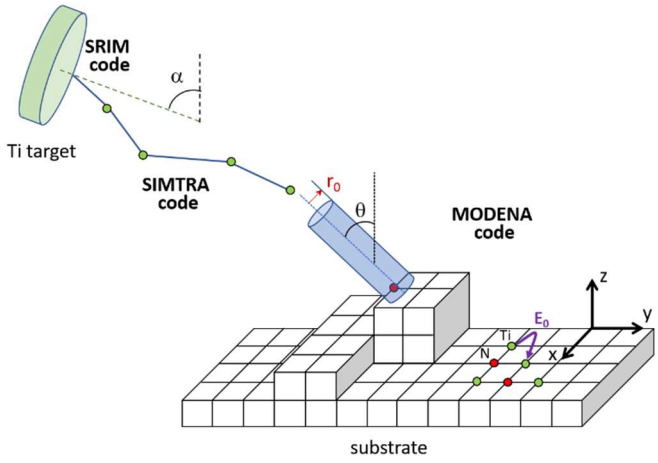

Figure 1: Schematics of the 3D growth model used for the kMC computer simulations of TiN film growth morphology at oblique angle incidence. The MODENA code uses a 3D cubic rigid lattice referred in the {x, y, z} frame, and includes both deposition and diffusion events. The particle trajectory from the target to the substrate is schematically shown in the picture for the case of MS conditions, where the incident angle θ of the particle reaching the substrate is taken from the angular distribution obtained from SIMTRA code (see Fig. 2), and may differ from the geometrical angle α between the target and substrate normals. Note that for the CF conditions, θ=α for all particles. Also shown in the picture are the radius r_0 of the cylinder inside which possible available deposition sites are selected, and the energy barrier E_0 for the diffusing particle (Ti or N single atom) on the terrace.

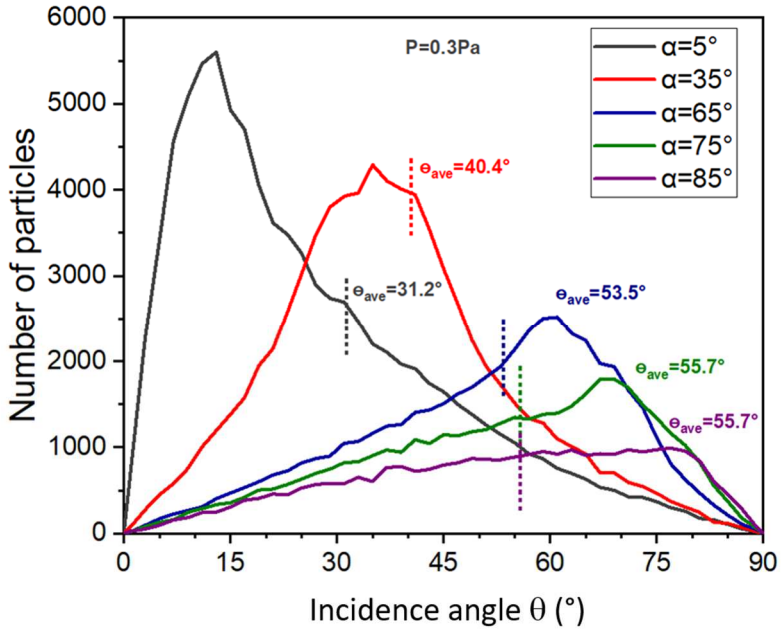

Figure 2: Angular distribution F(θ) of the particles reaching the substrate positioned at different inclination angles α in the range 5 to 85°, as computed from SIMTRA code at 0.3 Pa and considering the specific geometry of the MS deposition chamber used for the experiments. Vertical dashed lines indicate the average incidence angle θ_{ave} for each α condition.

The growth morphologies of TiN layers predicted by the MODENA simulator were benchmarked against those obtained experimentally on magnetron sputter-deposited TiN films under oblique angle geometry. The films, 1 μm thick, were deposited on Si substrates

using an Ar+N_2 plasma discharge, in a high-vacuum deposition chamber equipped with planar magnetron sources. Custom-made substrate holders were used to vary the inclination angle α of the substrate with respect to the Ti target. More details on the substrate configuration and chamber geometry can be found elsewhere [46]. The total working pressure was fixed at 0.3 Pa, and the Ti target operated in metallic mode (i.e. at a low N_2 partial pressure) using a dc power supply (300 W). The substrate was either left unheated (T= 300 K) or heated at 520 and 720 K using a resistive heater.

3. Results

3.1 Growth morphology of TiN films

The growth morphologies of TiN thin films computed at T=300, 400 and 500 K are shown in Figure 3 for the CF and MS conditions. The displayed snapshots are cross-sectional views in the (y, z) plane of the layer density projected along x, with color scale ranging from black (density=0) to white (density=1). This representation has the advantage of distinguishing better the column boundaries. Independently of the substrate temperature, the simulated films exhibit the formation of individual columns with high aspect ratio for α≥35°. The columns are tilted with respect to the substrate normal and oriented towards the incoming particle flux. As the substrate inclination angle α increases, the columns are more tilted and better defined but the deposited TiN layer is less and less dense. Note that at α=5°, column boundaries are not discernible, the TiN films are found to be very compact.

Comparing the effect of the angular distribution of the particle flux on the simulated thin film morphology, we can conclude that the columns are better defined and more tilted for the CF case. There is also a significant difference in the porosity of the TiN layers, as darker images (lower density) are observed in the CF case. However, the size of the columns is larger (almost twice) for the case of the MS distribution.

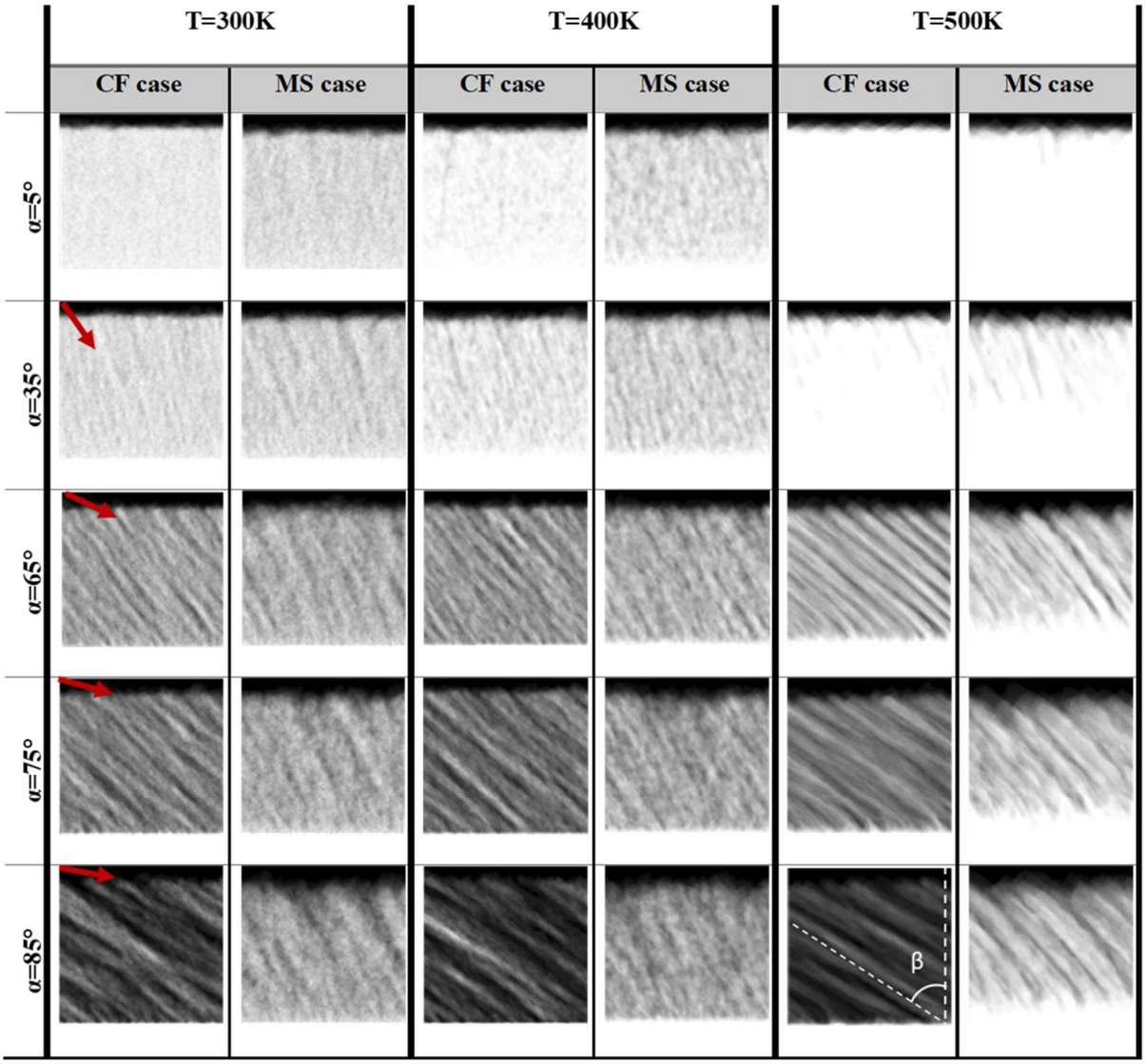

Figure 3: Cross-sectional views (in the (y,z) plane) of the computed TiN growth morphology for the CF and MS conditions at different substrate temperatures T and inclination angle α. The gray-level contrast reflects the layer density projected along the x direction. The red arrow on the left indicates the direction of the incoming flux.

In addition, morphological changes are observed when varying the substrate temperature. By increasing the temperature from 300 to 500 K, the columns become more tilted, but also appear denser and larger. In the CF case, the columns extend over the entire layer thickness, while when considering the MS distribution at 0.3 Pa one can observe that a dense region is

formed at the interface with the substrate and the thickness of this dense interlayer increases with the substrate temperature (see the bright contrast region in Figure 3).

Finally, we can also notice for $\alpha \geq 65°$ that the column tilt angles tend to increases with increasing film thickness. This bending effect is more pronounced at higher temperature (500 K) and for the MS case. It will be further discussed in Section 4.

3.2. Evolution of column tilt angle β

Figure 4 summarizes the results on the evolution of the column tilt angle β with respect to the substrate temperature and inclination angle α for the two considered angular distributions. It is found that i) β increases with α and the inclination of the columns is larger for the CF case comparatively to the MS case, and ii) for both cases, β increases with substrate temperature T.

The range of accessible β values is significantly larger in the CF case, with β increasing almost linearly from 15-25° to 50-60° with increasing α in the 35-85° range. When considering the MS distribution, one can notice a saturation phenomenon for $\alpha \geq 65°$, as β values do not exceed 35°. This can be explained by the characteristics of the angular distribution of the particle flux F(θ) reaching the substrate at 0.3 Pa. As shown in Figure 2, F(θ) curves are very broad and the center of the distribution is almost unchanged for α values in the 65-85° range, with average incident angle θ_{ave} values of 55°. This means that despite the substrate being more inclined, particles arrive with essentially the same angular distribution due to scattering in the gas phase. This saturation effect is even more pronounced as the working pressure increases, as shown in our previous work [46].

When surface diffusion mechanisms become thermally activated, i.e. at T=400 and 500 K, an increase in β angle is observed. However, increasing the substrate temperature from 300 to 400 K leads to a marginal increase of only 1-2° for all inclination angles α. A further

increase to 500 K has a more pronounced effect, β values being overall shifted by 5 to 7° for the MS and CF distributions, respectively, compared to the values obtained at 400K.

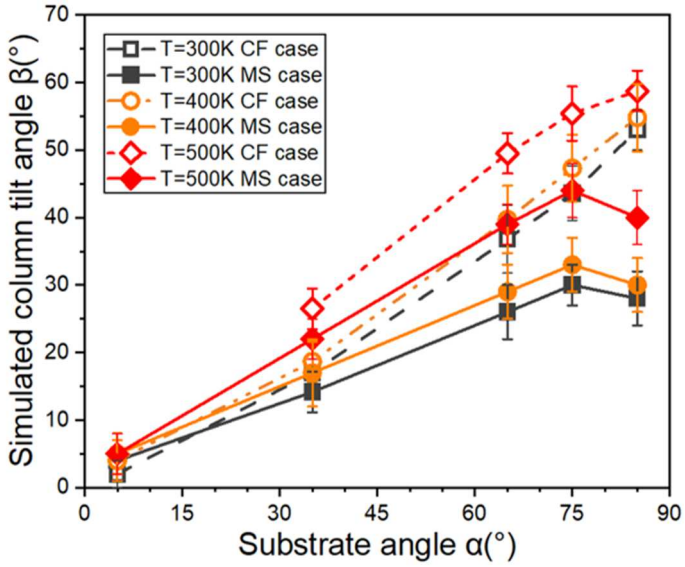

Figure 4: Dependence of the computed column tilt angle β on substrate temperature T and inclination angle α for the CF and MS deposition conditions.

3.3. Influence of temperature on the microstructure evolution

Figure 5 displays the evolution of the average layer density of the simulated TiN layers as a function of the substrate temperature and inclination angle for the two sets of simulations corresponding to CF and MS deposition conditions. The average layer density was computed taking into account the site occupancy in each layer, and the average performed throughout the bulk of the film, i.e., excluding the contributions from the substrate interface and film surface (growth front) regions. An example of the average layer density profile ρ(z) is shown in Figure 5a, plotted for the case α=75° and T = 400 K. For both deposition conditions, the depth profile evolution of the density allows to identify three regions: in the vicinity of the substrate, the interface region exhibiting the higher density, then the bulk of the film characterized by a constant density, and then the growth front region, characterized by a fast drop of the density down to zero. We can notice that the interface and surface regions are

more spread (almost twice) for the MS distribution. The plateau region reaches an average density of ~65% and 40% for the MS and CF case, respectively. This means that the TiN layers obtained using the MS angular distribution are denser, in qualitative agreement with the observations made from Figure 3 (compare the contrast in the simulations between the CF and MS cases). The ρ(z) profiles shown in Figure 5a also confirm a larger extent of the interface layer for the MS case, and the tendency to form columns with shorter lengths.

As shown in Figure 5b, the average layer density of the TiN layers decreases with increasing α, and this decrease is enhanced for collimated fluxes, especially for $\alpha > 35°$. In this latter case, the evolution approaches the limit given by the cosine law (plotted as a dashed line), which would traduce the loss of particles due to geometrical inclination of the substrate for a purely directional flux. For the MS case, the density decreases almost linearly for $\alpha \geq 35°$ with a similar slope for all temperatures. This is better illustrated in Fig. 5c in which computed data were normalized to the value obtained at $\alpha=5°$.

Increasing the substrate temperature leads to an increase of the layer density. This effect is visible and similar for both deposition conditions. A slight and constant offset (1%) of the average layer density is observed when T increases from 300 to 400 K, but densification is more pronounced at 500 K, particularly for the MS case for which a ~15% increase is observed. The trend depicted by the normalized data (Fig. 5c) reveals that the average layer density is weakly dependent on the temperature with increasing α, confirming that the shadowing effect is the main contribution of decrease in density at inclined substrate angles.

In addition, we can notice that the average layer density is higher for the CF case than for the MS case at low α angles, while this behavior is opposite at high α angles (see Fig. 5b). This cross-over phenomenon was also observed when considering the influence of the working pressure on the TiN growth morphologies obtained at room temperature [46],

suggesting that it is primarily governed by the angular distribution of the particle flux rather than by the substrate temperature.

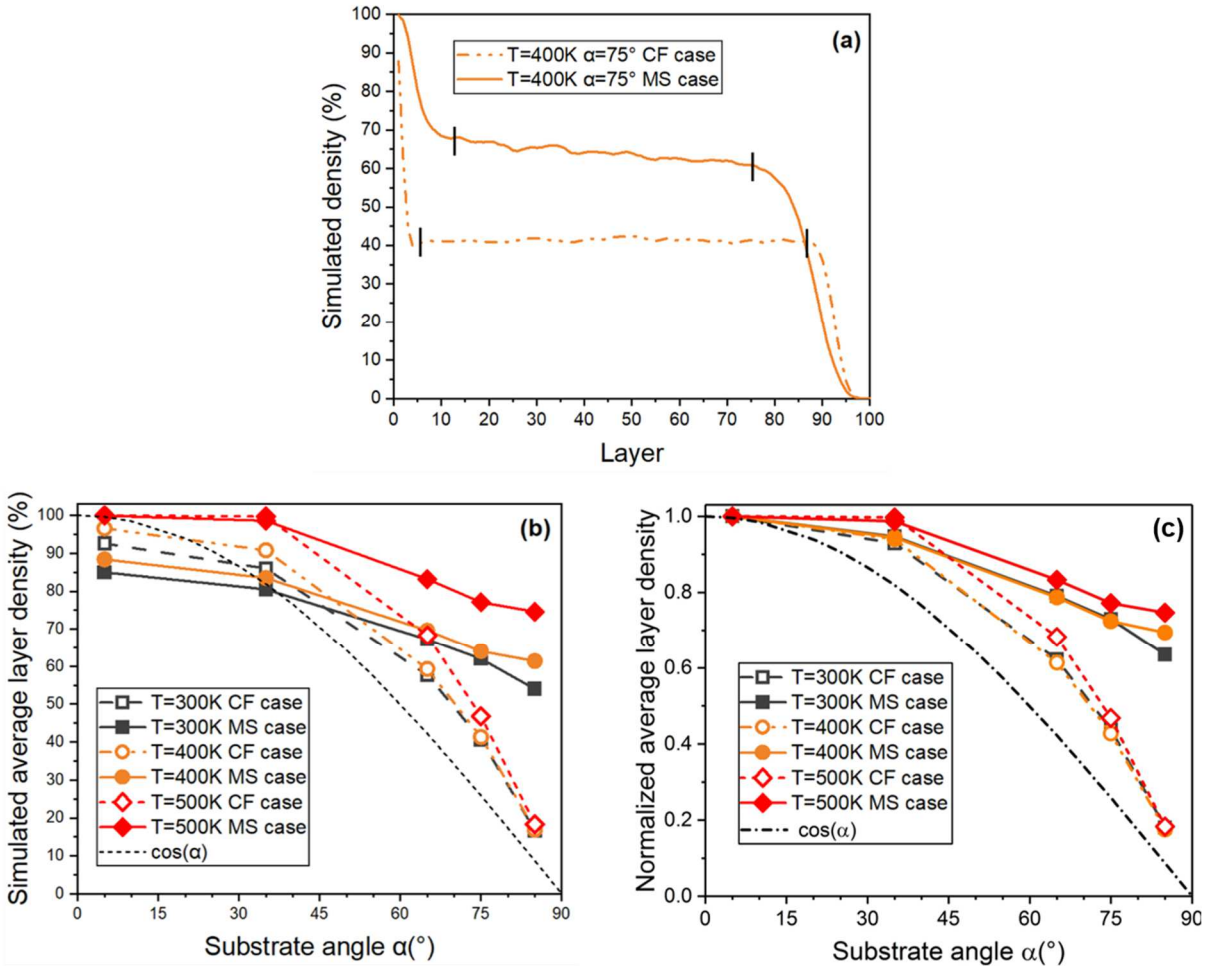

Figure 5: (a) Depth profile evolution of the average layer density ρ(z) of a TiN film deposited at α=75° and T=400K. (b) Evolution of the average layer density of TiN films with substrate temperature T and inclination angle α for the CF and MS deposition conditions. (c) same data as in (b) but normalized to the value computed at α=5°.

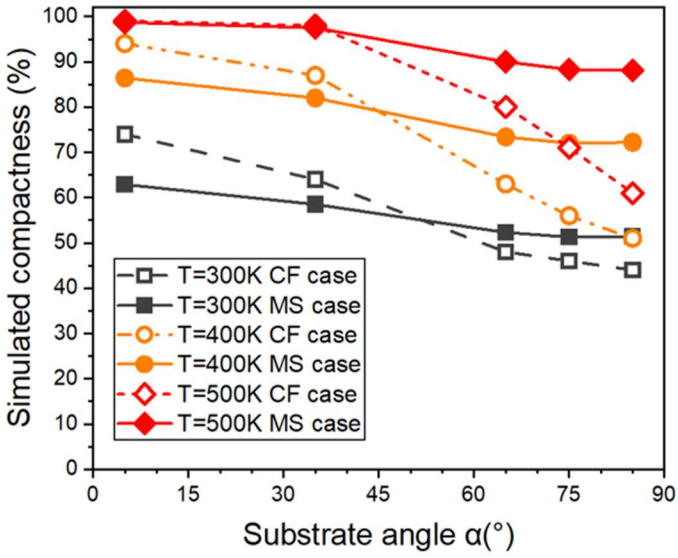

Figure 6: a) Evolution of the compactness of TiN films with substrate temperature T and inclination angle α for the CF and MS deposition conditions.

Figure 6 shows the evolution of the compactness parameter of the simulated TiN layers as a function of substrate temperature and inclination angle α for the two sets of simulations. The compactness increases with increasing temperature and decreases with increasing α angle. Like the evolution of the layer density shown in Figure 5, a cross-over phenomenon is observed when comparing the CF and MS angular distributions. Overall, the trend depicted by the compactness parameter is consistent with that revealed by the layer density: i) more porous layers are obtained at higher α angles, ii) surface diffusion promotes film densification, and iii) shadowing effect is exacerbated for directional particle fluxes (CF case). These results are consistent with (2D) kMC simulations performed by Yang *et al*. for Ni films [66].

Figure 7 plots the variations of the rms surface roughness ω versus substrate temperature T and inclination angle α. For both deposition conditions, the roughness increases with increasing substrate tilt angle. Between 300 and 400 K, ω increases slightly by 10 %. For T=300 and 500 K, TiN layers have the same roughness profile for α below 75° but one can

notice a decrease at 500 K and α=85°. This effect was confirmed by additional simulations performed using different initial seed values of the random number generator. Finally, one can note that the roughness is lower for the CF case for α ≤ 75° but becomes twice higher at α = 85° compared to the MS case.

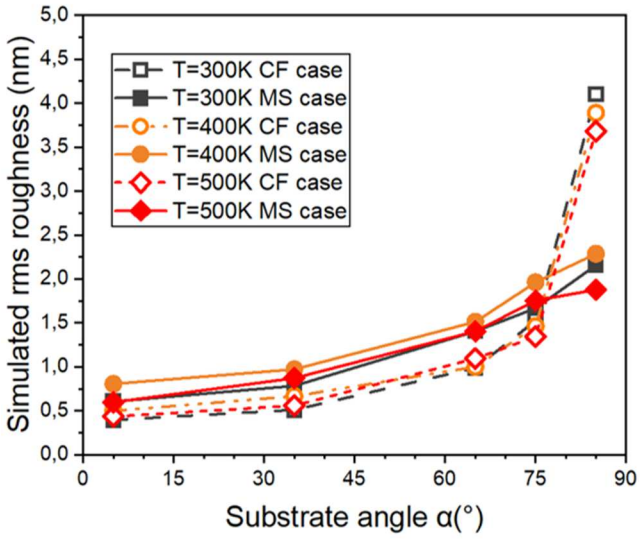

Figure 7: Evolution of the simulated rms roughness of TiN films with substrate temperature and inclination angle α for the CF and MS deposition conditions.

4. Discussion

4.1. Influence of the temperature on column tilt angle

In this section we compare the β values predicted by the MODENA simulator to experimental data and existing models reported in the literature. The comparison with experimental data is only shown after for the MS distribution since there are no available data for TiN films grown by thermal evaporation, i.e., under CF conditions. However, the trends predicted for the CF case by our model are in agreement with experimental data available for other materials [2,3,34,67].

4.1.1. β(α) relationship at T= 300 K

We first discuss the results obtained at T= 300 K, for which the growth is governed by atomic shadowing only since surface diffusion events are suppressed at this temperature. In the CF case (Figure 8a), it can be observed that the evolution of β follows with a good agreement the empirical tangent rule [30] at low substrate angle ($\alpha \leq 60°$) and the Tait's cosine law [31] at higher angle ($\alpha > 60°$). Such trend is commonly reported in the literature for many OAD films produced by thermal evaporation [2,3,67], although deviations exist depending on material type (elemental vs. compound) [34]. Note that the tangent rule is purely empirical and was derived by Nieuwenhuizen and Haanstra [30] from rudimentary observations of fractured surfaces of evaporated Al films, with no underlying physics behind. The cosine law is an analytical expression derived by Tait *et al*. [31] that further reproduced results obtained from 2D ballistic growth simulations of hard discs with limited surface diffusion (constrained to a single column) and restricted to evaporation (i.e., fixed angle of incidence α).

The trend observed for the CF case contrasts with results obtained for the MS distribution, see Figure 8b, for which β values lie below the tangent and cosine laws for $\alpha > 35°$. The β(α) evolution predicted by our kMC computations agrees fairly well with experimental β values obtained on MS deposited TiN films (see star symbols in Figure 8b), which validates the employed methodology.

As noticed before, a saturation phenomenon is observed at high α values for the MS case. Such finding is related to the angular broadening of the particle flux and short-range interaction of arriving particles with film surfaces (trapping mechanism) [33]. Both effects are relevant to MS deposition, and are also included in our kMC model. As shown in our previous work on TiN films obtained by combining OAD and MS [46], the particle flux is significantly broadened due to collision in the gas phase. The number of collisions increases from 12 at $\alpha=5°$ to 23 at $\alpha=85°$, according to SIMTRA calculations performed at 0.3 Pa for our

deposition geometry. For high α values the dispersion in θ is such that incoming particles reach the substrate/film surface from all possible angles. Figure 2 shows that the angular distribution is almost the same for $65° \leq \alpha \leq 85°$, which explains the saturation phenomenon observed in Figure 8b. This large dispersion in the incidence angle of the particles decrease the shadowing effect, resulting in deviations from the cosine and tangent laws. These findings have been reported by others, in particular the column tilt angle β is found to significantly decrease with increasing working pressure for sputter-deposited films at glancing angle incidence [41,68–70]. This was rationalized by Garcia-Martin *et al*. by introducing the concept of thermalization degree Ξ [36]. A value of $\Xi = 13.2 \times p_g L$ Pa^{-1} m^{-1} has been reported by Alvarez *et al*. [63] for Ti atoms colliding with Ar, which yields a value of $\Xi = 0.72$ for L=0.18 m and p_g=0.3 Pa, where p_g is the working pressure and L the target-to-substrate distance. According to the simulations reported by these authors [36], one would therefore expect a column tilt angle $\beta \sim 35°$ for $\Xi = 0.7$ and α= 85°, a value slightly higher than our experimental and computed value of $\beta = 27°$.

However, the Ξ parameter does not include any information on the flux directionality. We have shown in our previous study [46] that a more relevant quantity is to calculate the resultant incident angle, θ_{res}, as defined originally by Siad *et al*. [35]. Plotting β vs. θ_{res} provides then a more appropriate comparison with thermal evaporation and empirical laws derived originally for directional fluxes. Another possible explanation for this difference is the contribution of hyperthermal particles [63,71], which is expected to be significant for $\Xi <$ 1. Particles with relatively high kinetic energy, typically > 25 eV for TiN [72], will contribute to film densification by collision-induced atomic displacement or biased surface diffusion, with the consequence of straightening up the columns (referred as a dragging mechanism [63]).

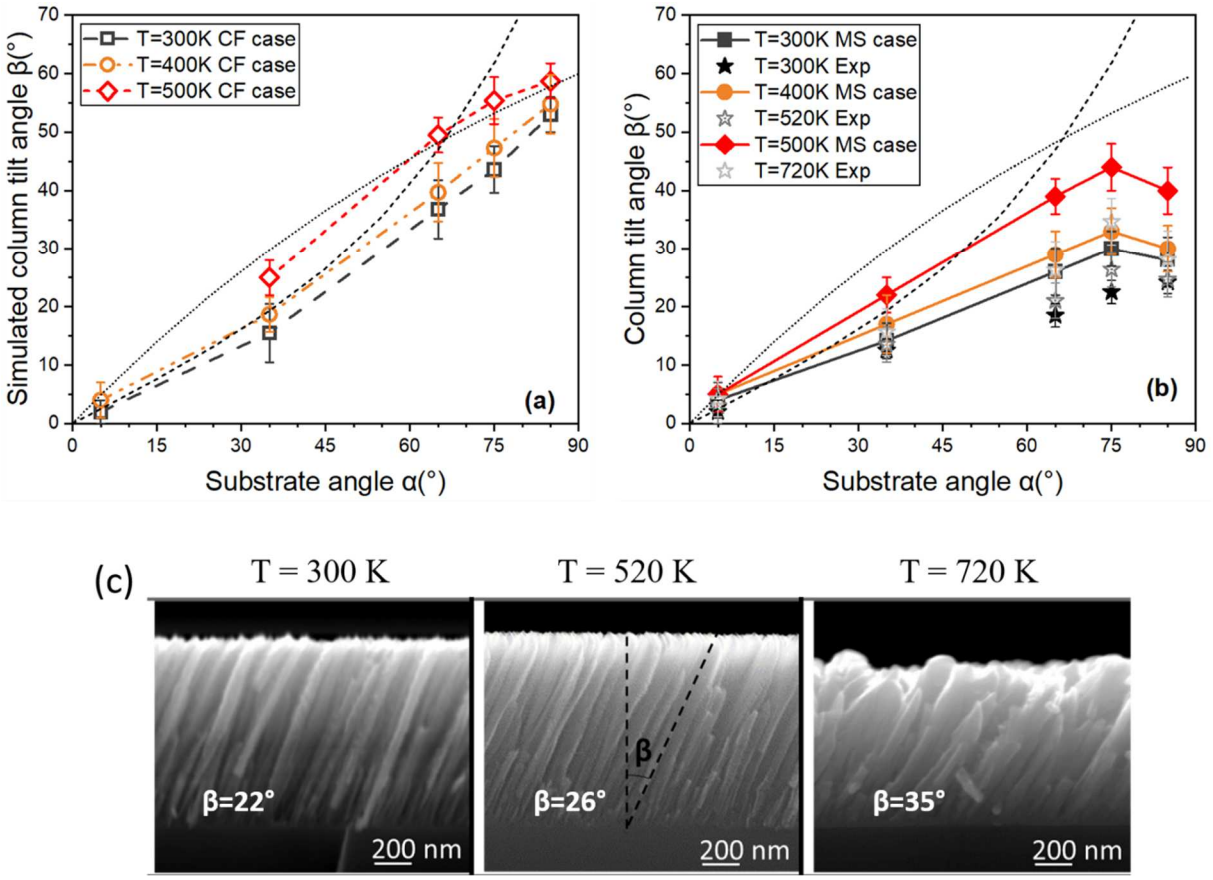

Figure 8: Influence of substrate temperature on the β vs. α evolution for TiN films obtained at OAD with (a) CF and (b) MS angular distribution. Experimental β values are compared to kMC predictions for the MS case. The cosine (short dotted line) and tangent (dashed line) laws are also displayed. (c) Cross-section scanning electron microscopy images of TiN films deposited by MS at α= 75° and different substrate temperatures.

4.1.2. Influence of surface diffusion (T ≥ 400 K)

Surface diffusion is a thermally-activated process by which mass transport leads to morphological and microstructural changes depending on the diffusion length-scale of adatoms. Under conventional (i.e. normal incidence) deposition conditions, the microstructure evolution is usually depicted as a function of the homologous temperature, $T_h = T/T_m$, where T_m is the melting point of the material, and qualitatively described by structure zone models (SZM) [73,74]. At OAD conditions, surface diffusion is expected to counteract atomic shadowing as it concurs to smoothening the film surface and reducing the porosity.

Mukherjee and Gall [75] have revisited SZM for glancing angle deposition (GLAD) conditions, and identified distinct regions for the formation of nanorods, faceted nanocolumns, protrusions and even whiskers with increasing T_h. Deniz *et al*. [10] have reported a temperature threshold above which nanorods can no longer be formed, and reported a threshold value of T_h~0.33 for elemental metals deposited at $\alpha = 80°$ with substrate rotation of 5 rpm.

When the substrate is kept stationary during OAD, the influence of substrate temperature on the column tilt angle β is far to be fully understood as opposite results have been reported in the literature depending on deposition conditions and film-substrate combinations: there are cases for which the column inclination is closer (i.e. a decrease in β) [38,39,41,76] or further away (i.e. an increase in β) [29,37,40,44] from the substrate normal with increasing T. The first observation is typically encountered for low-T_m material/large surface diffusivities (e.g., Mg [76]), while the latter is seen for high-T_m material/low surface diffusivity (e.g., Mo or Ta [37]). In the work by Dervaux *et al*. [41] on GLAD Ti films, a decrease in β was found with increasing temperature but the effect was the most pronounced between 723 and 823 K ($0.37 \leq T_h \leq 0.45$), i.e. corresponding to zone II of the SZM. Different mechanisms are invoked to explain one or another β(T) dependency. By virtue of Fick's first law of diffusion, there is a driving force for mass transport from the column tip (high adatom density) towards the valleys of the shadowed region (low adatom density). An increased surface diffusion will thus eliminate high-curvature features on the surface, smearing out self-shadowing effect, and leading to a decrease of β. The increase of β with temperature is contributed either to the competition between random and directionally-biased surface diffusion [29,44] or to a change in nucleation conditions, as proposed by Elofsson *et al*. [40].

The present findings on simulated TiN film morphology show an increase in β with increasing temperature in the 300-500 K range for both deposition modes. For instance, the magnitude of this increase is ~12° at α = 75° and ~7° at α = 85° for the CF case, and ~13° for the MS case for these two α angles (see Figure 8). This trend is in qualitative agreement with our experimental observation on MS-OAD TiN films for which columns were found to be more inclined with increasing substrate temperature: e.g., β increases from 22° at 300 K to 35° at 720 K (see Figure 8b and 8c). Note that the T_h range investigated in this work corresponds to 0.10-0.22, i.e., to zone I/zone T of SZM, so that the results obtained for TiN appear consistent with the trend observed for low-mobility materials.

Our numerical simulations were run without taking into account explicitly the kinetic energy of the incoming particles, so that the biased surface diffusion (with conservation of the momentum parallel to the surface) is not contributing to the morphological evolution of the TiN columns. A closer inspection to the early stages of growth (see Figure 9) clearly shows that at higher substrate temperature (T= 500 K), the film consists of large, separated islands comparatively to the situation at 300 K for which adatoms hit and stick on the original deposition sites leading to a surface relief with a stochastic roughness. A lower nuclei density is therefore found at T=500 K, leading to larger and more inclined columns upon further film thickening due to shadowing. These observations are consistent with the model proposed by Elofsson *et al*. [40] in which the range of accessible β values depends on the separation length to island radius ratio, and would suggest that nucleation conditions are an important factor in controlling the column tilt angle β of TiN films characterized by relatively low surface self-diffusivities.

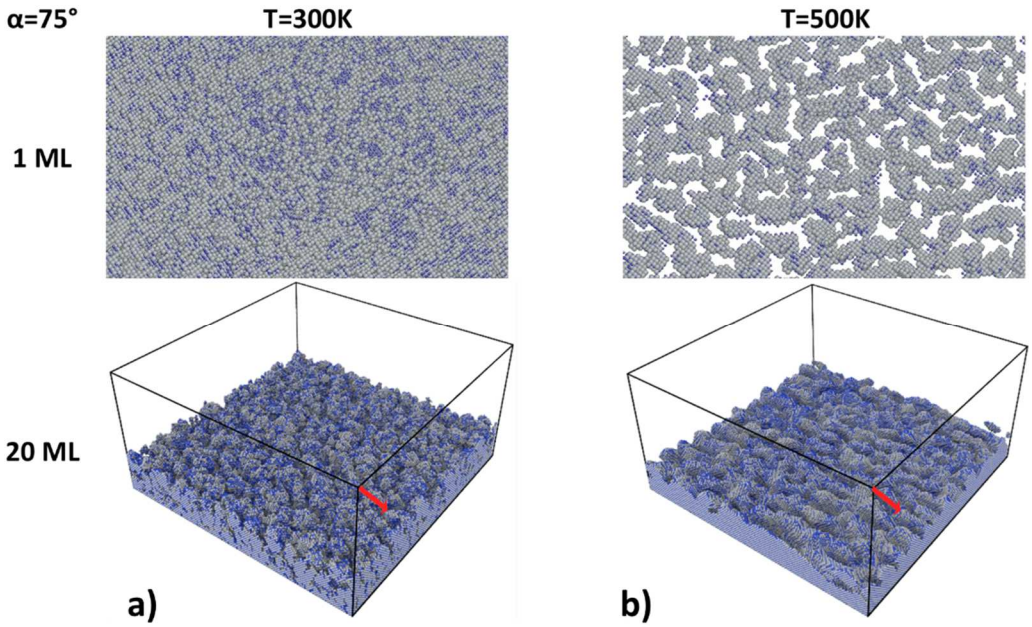

Figure 9: Snapshots of the TiN film morphology in the early growth stages (corresponding to a nominal thickness of 1 and 20 ML) computed for the MS case at a substrate inclination angle α=85° and (a) T= 300 K and (b) T = 500 K. The red arrow shows the direction of the incoming particle flux.

4.2. 3D morphology of TiN nanocolums: broadening, bending and bundling phenomena

We now discuss some specific morphological features that developed with increasing film thickness. These include column broadening and bending, as well as their merging in the direction perpendicular to the incident flux, a phenomenon often referred as bundling association or fanning [1,77,78]. These anisotropic 3D features are commonly observed in most OAD films including metal and oxides [1,3,20,78], and were here consistently reproduced for the case of TiN by the MODENA simulator.

Column extinction and broadening is an intrinsic phenomenon of the growth at oblique angle incidence. Close to the film/substrate interface, the density of columns is relatively high and depends on the nucleation conditions that are primarily affected by deposition rate and substrate temperature [79]. It can be observed that with increasing T, the film density at the

3D growth morphology of TiN films at T=500 K	
CF case	MS case

interface is higher (see cross-section images of Figure 2 and layer density profiles in Figure 5). The increased surface diffusion at T=500 K allows adatoms to diffuse from the top of the columns downwards, filling and densifying the interface area and thus reducing the shadowing effect. As the growth proceeds, the shadowing mechanism prevails and engenders a high rate of column extinction as taller features of the surface relief capture an ever-larger fraction of the incoming flux and continue to grow at the expense of neighboring features. The surviving columns will therefore broaden with increasing film thickness. The kMC simulations (see cross-section images taken in the (y,z) planes in Figure 10) show that the width of the TiN columns is twice larger for the MS case compared to the CF case, which shows the importance of the angular dispersion of the particle flux in governing the cross-sectional increase of the columns. Similar conclusions were reported by Alvarez *et al*. for TiO_2 films [57]. For the case of TiN, due to limited surface diffusion even at T=500 K, no significant column broadening could be observed with increasing film thickness (see Figure 10). Although the finite size of the simulation box along the z direction may limit the development of such phenomenon, the kMC results are in qualitative agreement with experimental observations, for which effective column broadening was only observed at higher temperature (T= 720 K), see Figure 8c.

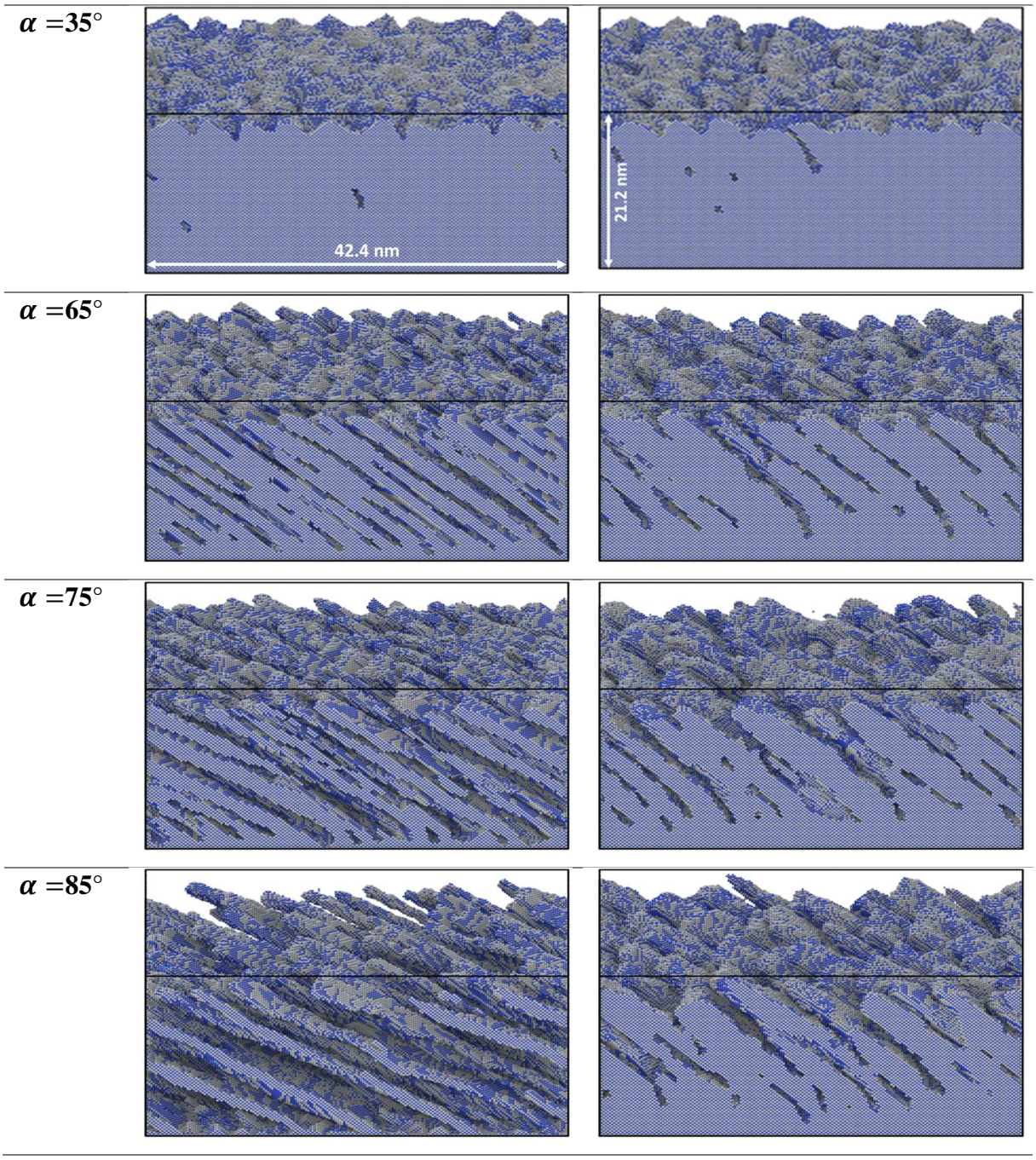

Figure 10: Cross-sectional (y,z) and surface (x,y) views of the TiN growth morphology computed at T= 500 K and different substrate inclination angles. The CF and MS cases are displayed on the left and right panel, respectively.

However, a noticeable feature is that the TiN columns tend to bend further in the direction of the incoming flux as the films grow thicker, i.e., β increases with increasing film

thickness. This phenomenon is enhanced at higher temperature and for the MS case, suggesting importance of both thermally activated self-diffusion processes and flux profile. For instance, we can note for the TiN film deposited at $\alpha = 85°$ and T=300 K an increase in the inclination of the columns from the substrate interface to the film surface by about 1.6°, while this increase in β reaches 2.3 and 8.3° at T=400 K and 500 K, respectively. Growth simulations performed at T= 573 K confirm this bending for TiN, ZrN and HfN films [80].

So far, we have discussed the growth morphology in the incidence plane (y,z). However, due to the anisotropic nature of the shadowing mechanism, in the direction perpendicular to the incidence plane (i.e., transverse direction along x), the growth conditions remain the same as for normal incidence and coalescence between columns is likely to occur. Under certain conditions of substrate inclination and temperature, the columns exhibit a gradual lateral fanning and can eventually merge in the transverse direction, forming a flake-like structure [20,74,77]. In the case of TiN films [53], such elongated patterns were successfully reproduced by the MODENA simulator for inclination angles in the 60-75° range. At $\alpha = 85°$, the increase of porosity leads to a larger separation between columns, which prevents the occurrence of column merging. As seen in Figure 11, the aggregation of columns forms an elongated zig-zag structure in the direction perpendicular to the incoming flux for the CF case. The connectivity between columns is enhanced at higher substrate temperature. For the MS case, the bundling phenomenon is only observed at T = 500 K, and the columns develop more spherical cross-sections. This is contributed to the more isotropic angular distribution of the particle flux for the MS mode, especially along the azimuthal direction, which favors lateral attachment of particles (at the sides of the columns). Lopez-Santos *et al.* [77] have shown that the anisotropic widening of columns in the transverse direction is the result of a competition between surface shadowing and surface trapping processes. They concluded that higher surface trapping efficiencies promoted the bundling association of columns. However,

their growth simulations were restricted to thermal evaporation at low substrate temperature conditions. The results obtained in the present study also demonstrate the importance of surface diffusion and angular distribution of the particle flux in the formation of coalescent domains extending in the transverse direction.

Our findings confirm that there exists a window of deposition process parameters leading to OAD films with anisotropic microstructures related to the widening, and ultimately the merging, of columns along the transverse direction. This has direct consequences on the anisotropy of the films' properties, e.g., the refractive index of oxide materials [20,81], the electrical resistivity or the propagation of elastic waves, as reported recently by Chargui *et al*. [69] in W GLAD films.

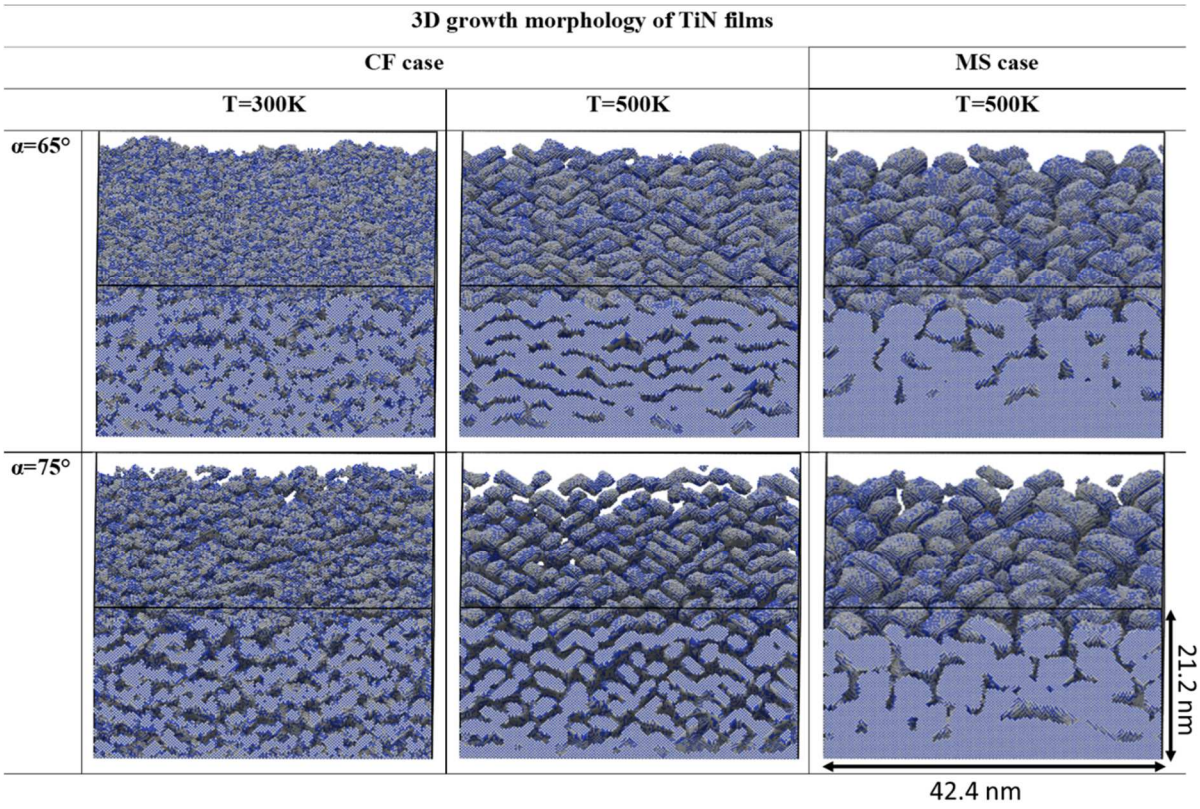

Figure 11: Cross-sectional (x,z) and surface (y,x) views of the TiN growth morphology illustrating the nanocolumn bundling phenomenon observed at α = 65° and 75° for the CF case at T= 300 K (left panel) and 500 K (central panel), and for the MS case at T= 500 K (right panel).

5. Conclusions

In this work we have studied using kMC-based atomistic simulations the 3D growth morphology and microstructure development of TiN films deposited at various substrate inclination angles α. The current scheme allows transport modelling of neutral species in the gas phase, combined with deposition and diffusion events of both N and Ti species on a rigid lattice. We varied the substrate temperature and angular distribution of the particle flux to critically examine their influence on the column inclination angle β, film porosity and surface topography. The growth morphology predicted by the MODENA simulator is in agreement with experimental observations obtained on sputter-deposited TiN films. In particular, the numerical simulations correctly reproduce the saturation phenomenon of the column inclination angle observed for magnetron sputtering conditions, while growth conditions involving collimated fluxes lead to a gradual increase of β with increasing α that closely follows the $\beta(\alpha)$ cosine law at high α values ($> 60°$).

We demonstrate the importance of surface diffusion processes in governing both the inclination of columns and their association in the form of bundles in the direction perpendicular to the particle flux. The increase of β with substrate temperature in the range 300-500 K is contributed to a lower nucleation density, as revealed from inspection of the computed early growth stages. Experimental findings confirm larger β values for TiN films with increasing temperatures from 300 to 720 K, similarly to what has been observed for other low-mobility materials like Cr, Mo or Ta, while a straightening of the columns is often reported for high-mobility materials.

The growth model developed here for the case of TiN system can be readily implemented to predict the growth morphology of other transition metal nitrides or oxides with cubic rock-

salt structure. The proposed multi-scale numerical modelling can serve as a virtual coater to better understand the fundamental aspects of film nucleation and growth, and to select the optimum process parameters, from a broad range of deposition conditions, to tailor the desired morphologies of nanostructures produced by oblique angle deposition for specific applications.

Acknowledgments

This work partially pertains to the French Government program “Investissements d’Avenir” (LABEX INTERACTIFS, reference ANR-11-LABX-0017-01). RM acknowledges the French Ministry for Europe and Foreign Affairs for granting him a scholarship through the Campus France - Eiffel Excellence Program (contract 919884J), as well as the Conférence des Présidents d’Université (CPU) for financial support.

Data Availability

The raw/processed data required to reproduce these findings cannot be shared at this time as the data also forms part of an ongoing study.

References

[1] H. van Kranenburg, C. Lodder, Tailoring growth and local composition by oblique-incidence deposition: a review and new experimental data, Mater. Sci. Eng. R Reports. 11 (1994) 295–354.

[2] M.M. Hawkeye, M.J. Brett, Glancing angle deposition: Fabrication, properties, and applications of micro- and nanostructured thin films, J. Vac. Sci. Technol. A Vacuum, Surfaces, Film. 25 (2007) 1317–1335. doi:10.1116/1.2764082.

[3] A. Barranco, A. Borras, A.R. Gonzalez-Elipe, A. Palmero, Perspectives on oblique angle deposition of thin films: From fundamentals to devices, Prog. Mater. Sci. 76 (2016) 59–153. doi:10.1016/j.pmatsci.2015.06.003.

[4] Y.-J. Jen, C.-F. Lin, Anisotropic optical thin films finely sculptured by substrate sweep technology, Opt. Express. 16 (2008) 5372–5377. doi:10.1364/oe.16.005372.

[5] S.K. Sharma, D.Y. Kim, Abnormal residual stress in nanostructured al thin films grown on Ti/glass substrates, Curr. Appl. Phys. 13 (2013) 1874–1879. doi:10.1016/j.cap.2013.07.022.

[6] M.J.M. Jimenez, V. Antunes, S. Cucatti, A. Riul, L.F. Zagonel, C.A. Figueroa, D. Wisnivesky, F. Alvarez, Physical and micro-nano-structure properties of chromium nitride coating deposited by RF sputtering using dynamic glancing angle deposition, Surf. Coatings Technol. 372 (2019) 268–277. doi:10.1016/j.surfcoat.2019.05.023.

[7] R. Daniel, M. Meindlhumer, W. Baumegger, J. Todt, J. Zalesak, T. Ziegelwanger, C. Mitterer, J. Keckes, Anisotropy of fracture toughness in nanostructured ceramics controlled by grain boundary design, Mater. Des. 161 (2019) 80–85. doi:10.1016/J.MATDES.2018.11.028.

[8] L. Chen, L. Andrea, Y.P. Timalsina, G.C. Wang, T.M. Lu, Engineering epitaxial-nanospiral metal films using dynamic oblique angle deposition, Cryst. Growth Des. 13 (2013) 2075–2080. doi:10.1021/cg400142g.

[9] C.M. Zhou, H.F. Li, D. Gall, Multi-component nanostructure design by atomic shadowing, Thin Solid Films. 517 (2008) 1214–1218. doi:10.1016/j.tsf.2008.05.049.

[10] D. Deniz, R.J. Lad, Temperature threshold for nanorod structuring of metal and oxide films grown by glancing angle deposition, J. Vac. Sci. Technol. A Vacuum, Surfaces, Film. 29 (2011) 11020. doi:10.1116/1.3525882.

[11] K. Yatsugi, K. Nishikawa, Highly anisotropic titanium nitride nanowire arrays for low-loss hyperbolic metamaterials fabricated via dynamic oblique deposition, Nanotechnology. 30 (2019) 335705.

[12] C.M. Zhou, D. Gall, Branched Ta nanocolumns grown by glancing angle deposition, Appl. Phys. Lett. 88 (2006) 203117. doi:10.1063/1.2204759.

[13] J. Wang, H. Huang, S. V. Kesapragada, D. Gall, Growth of Y-shaped nanorods through physical vapor deposition, Nano Lett. 5 (2005) 2505–2508. doi:10.1021/nl0518425.

[14] D.J. Poxson, F.W. Mont, M.F. Schubert, J.K. Kim, E.F. Schubert, Quantification of porosity and deposition rate of nanoporous films grown by oblique-angle deposition, Appl. Phys. Lett. 93 (2008) 101914. doi:10.1063/1.2981690.

[15] A. Singh, A. Sharma, M. Tomar, V. Gupta, Tunable nanostructured columnar growth of SnO2 for efficient detection of CO gas, Nanotechnology. 29 (2018) 65502. doi:10.1088/1361-6528/aa9bc0.

[16] X. Xu, M. Arab Pour Yazdi, J.B. Sanchez, A. Billard, F. Berger, N. Martin, Exploiting the dodecane and ozone sensing capabilities of nanostructured tungsten oxide films, Sensors Actuators, B Chem. 266 (2018) 773–783. doi:10.1016/j.snb.2018.03.190.

[17] J.Q. Xi, M.F. Schubert, J.K. Kim, E.F. Schubert, M. Chen, S.Y. Lin, W. Liu, J.A. Smart, Optical thin-film materials with low refractive index for broadband elimination of Fresnel reflection, Nat. Photonics. 1 (2007) 176–179. doi:10.1038/nphoton.2007.26.

[18] J. Parra-Barranco, M. Oliva-Ramirez, L. Gonzalez-Garcia, M. Alcaire, M. Macias-Montero, A. Borras, F. Frutos, A.R. Gonzalez-Elipe, A. Barranco, Bending induced self-organized switchable gratings on polymeric substrates, ACS Appl. Mater. Interfaces. 6 (2014) 11924–11931. doi:10.1021/am5037687.

[19] H. Ferhati, F. Djeffal, N. Martin, Highly improved responsivity of self-powered UV–Visible photodetector based on TiO2/Ag/TiO2 multilayer deposited by GLAD technique: Effects of oriented columns and nano-sculptured surface, Appl. Surf. Sci. 529 (2020) 35–38. doi:10.1016/j.apsusc.2020.147069.

[20] F. Maudet, B. Lacroix, A.J. Santos, F. Paumier, M. Paraillous, S. Hurand, A. Corvisier, C. Marsal, B. Giroire, C. Dupeyrat, R. García, F.M. Morales, T. Girardeau, Optical and nanostructural insights of oblique angle deposited layers applied for photonic coatings, Appl. Surf. Sci. 520 (2020) 146312. doi:10.1016/j.apsusc.2020.146312.

[21] N. N. Kariuki, W. J. Khudhayer, T. Karabacak, D. J. Myers, GLAD Pt–Ni Alloy Nanorods for Oxygen Reduction Reaction, ACS Catal. 3 (2013) 3123–3132. doi:10.1021/cs400759u.

[22] M.D. Gasda, R. Teki, T.-M. Lu, N. Koratkar, G.A. Eisman, D. Gall, Sputter-Deposited Pt PEM Fuel Cell Electrodes: Particles vs Layers, J. Electrochem. Soc. 156 (2009) B614. doi:10.1149/1.3097188.

[23] W.J. Khudhayer, A.U. Shaikh, T. Karabacak, Periodic Pt nanorod arrays with controlled porosity for oxygen reduction reaction, Nanosci. Nanotechnol. Lett. 4 (2012) 999–1007. doi:10.1166/nnl.2012.1439.

[24] E. Haye, A. Achour, A. Guerra, F. Moulaï, T. Hadjersi, R. Boukherroub, A. Panepinto, T. Brousse, J.J. Pireaux, S. Lucas, Achieving on chip micro-supercapacitors based on CrN deposited by bipolar magnetron sputtering at glancing angle, Electrochim. Acta. 324 (2019) 134890. doi:10.1016/j.electacta.2019.134890.

[25] Z. Qi, B. Wei, J. Wang, Y. Yang, Z. Wang, Nanostructured porous CrN thin films by oblique angle magnetron sputtering for symmetric supercapacitors, J. Alloys Compd. 806 (2019) 953–959. doi:10.1016/j.jallcom.2019.07.325.

[26] P.W. Chi, C.W. Su, D.H. Wei, Control of hydrophobic surface and wetting states in ultra-flat ZnO films by GLAD method, Appl. Surf. Sci. 404 (2017) 380–387. doi:10.1016/j.apsusc.2017.01.266.

[27] U. Allenstein, E.I. Wisotzki, C. Gräfe, J.H. Clement, Y. Liu, J. Schroers, S. G. Mayr, Binary Fe-Pd submicron structures fabricated through glancing angle deposition (GLAD) for bioapplications, Mater. Des. 131 (2017) 366–374.

doi:10.1016/j.matdes.2017.06.032.

[28] D. Vick, L.J. Friedrich, S.K. Dew, M.J. Brett, K. Robbie, M. Seto, T. Smy, Self-shadowing and surface diffusion effects in obliquely deposited thin films, Thin Solid Films. 339 (1999) 88–94. doi:10.1016/S0040-6090(98)01154-7.

[29] L. Abelmann, C. Lodder, Oblique evaporation and surface diffusion, Thin Solid Films. 305 (1997) 1–21. doi:10.1016/S0040-6090(97)00095-3.

[30] J.M. Nieuwenhuizen, H.B. Haanstra, Microfractography of thin films, Philips Tech. Rev. 27 (1966) 87–91.

[31] R. Tait, T. Smy, M. Brett, Modeling and Characterization of Columnar Growth in Evaporated-Films, Thin Solid Films. 226 (1993) 196–201. doi:10.1016/0040-6090(93)90378-3.

[32] B. Tanto, G. Ten Eyck, T.M. Lu, A model for column angle evolution during oblique angle deposition, J. Appl. Phys. 108 (2010) 26107. doi:10.1063/1.3465296.

[33] R. Alvarez, C. Lopez-Santos, J. Parra-Barranco, V. Rico, A. Barranco, J. Cotrino, A.R. Gonzalez-Elipe, A. Palmero, Nanocolumnar growth of thin films deposited at oblique angles: Beyond the tangent rule, J. Vac. Sci. Technol. B, Nanotechnol. Microelectron. Mater. Process. Meas. Phenom. 32 (2014) 41802. doi:10.1116/1.4882877.

[34] H. Zhu, W. Cao, G.K. Larsen, R. Toole, Y. Zhao, Tilting angle of nanocolumnar films fabricated by oblique angle deposition, J. Vac. Sci. Technol. B. 30 (2012) 30606. doi:10.1116/1.4710999.

[35] A. Siad, A. Besnard, C. Nouveau, P. Jacquet, Critical angles in DC magnetron glad thin films, Vacuum. 131 (2016) 305–311. doi:10.1016/j.vacuum.2016.07.012.

[36] J.M. García-Martín, R. Alvarez, P. Romero-Gómez, A. Cebollada, A. Palmero, Tilt angle control of nanocolumns grown by glancing angle sputtering at variable argon pressures, Appl. Phys. Lett. 97 (2010) 173103. doi:10.1063/1.3506502.

[37] S. Liedtke, C. Grüner, J.W. Gerlach, B. Rauschenbach, Comparative study of sculptured metallic thin films deposited by oblique angle deposition at different temperatures, Beilstein J. Nanotechnol. 9 (2018) 954–962. doi:10.3762/bjnano.9.89.

[38] N.G. Nakhodkin, A.I. Shaldervan, Effect of vapour incidence angles on profile and properties of condensed films, Thin Solid Films. 10 (1972) 109–122. doi:10.1016/0040-6090(72)90276-3.

[39] T. Hashimoto, K. Okamoto, K. Hara, M. Kamiya, H. Fujiwara, Columnar structure and texture of iron films evaporated at oblique incidence, Thin Solid Films. 91 (1982) 145–154. doi:10.1016/0040-6090(82)90428-X.

[40] V. Elofsson, D. Magnfält, M. Samuelsson, K. Sarakinos, Tilt of the columnar microstructure in off-normally deposited thin films using highly ionized vapor fluxes, J. Appl. Phys. 113 (2013) 174906. doi:10.1063/1.4804066.

[41] J. Dervaux, P.A. Cormier, P. Moskovkin, O. Douheret, S. Konstantinidis, R. Lazzaroni, S. Lucas, R. Snyders, Synthesis of nanostructured Ti thin films by combining glancing angle deposition and magnetron sputtering: A joint experimental and modeling study, Thin Solid Films. 636 (2017) 644–657. doi:10.1016/j.tsf.2017.06.006.

[42] S. Müller-Pfeiffer, H. van Kranenburg, J.C. Lodder, A two-dimensional Monte Carlo

model for thin film growth by oblique evaporation: simulation of two-component systems for the example of Co□Cr, Thin Solid Films. 213 (1992) 143–153. doi:10.1016/0040-6090(92)90489-X.

[43] S. Lichter, L. Chen, Model for columnar microstructure of thin solid films, Phys. Rev. Lett. 56 (1986) 1396–1399.

[44] K. Hara, M. Kamiya, T. Hashimoto, K. Okamoto, H. Fujiwara, Oblique-incidence anisotropy of the iron films evaporated at low substrate temperatures, J. Magn. Magn. Mater. 73 (1988) 161–166. doi:10.1016/0304-8853(88)90286-7.

[45] F. Nita, C. Mastail, G. Abadias, Three-dimensional kinetic Monte Carlo simulations of cubic transition metal nitride thin film growth, Phys. Rev. B. 93 (2016) 64107. doi:10.1103/PhysRevB.93.064107.

[46] B. Bouaouina, C. Mastail, A. Besnard, R. Mareus, F. Nita, A. Michel, G. Abadias, Nanocolumnar TiN thin film growth by oblique angle sputter-deposition: Experiments vs. simulations, Mater. Des. 160 (2018) 338–349. doi:10.1016/j.matdes.2018.09.023.

[47] S. Venkataramanababu, G. Nair, P. Deshpande, M.A. Jithin, S. Mohan, A. Ghosh, Chiro-Plasmonic Refractory Metamaterial with Titanium Nitride (TiN) Core-Shell Nanohelices, Nanotechnology. 29 (2018) 255203.

[48] P. Patsalas, N. Kalfagiannis, S. Kassavetis, Optical properties and plasmonic performance of titanium nitride, Materials (Basel). 8 (2015) 3128–3154. doi:10.3390/ma8063128.

[49] Y.-J. Jen, W.-C. Wang, K.-L. Wu, M.-J. Lin, Extinction Properties of Obliquely Deposited TiN Nanorod Arrays, Coatings. 8 (2018) 465. doi:10.3390/coatings8120465.

[50] Y.J. Jen, K. Bin Yang, P.C. Lin, M.H. Chung, Deposited ultra-thin titanium nitride nanorod array as a plasmonic near-perfect light absorber, Sci. Rep. 10 (2020) 22269. doi:10.1038/s41598-020-79399-4.

[51] A. Kharitonov, S. Kharintsev, Tunable optical materials for multi-resonant plasmonics: from TiN to TiON [Invited], Opt. Mater. Express. 10 (2020) 513–531. doi:10.1364/ome.382160.

[52] S. Ishii, S.L. Shinde, T. Nagao, Nonmetallic Materials for Plasmonic Hot Carrier Excitation, Adv. Opt. Mater. 7 (2019) 1800603. doi:10.1002/adom.201800603.

[53] S. Mahieu, P. Ghekiere, G. De Winter, R. De Gryse, D. Depla, G. Van Tendeloo, O.I. Lebedev, Biaxially aligned titanium nitride thin films deposited by reactive unbalanced magnetron sputtering, Surf. Coatings Technol. 200 (2006) 2764–2768. doi:10.1016/J.SURFCOAT.2004.09.012.

[54] G. Abadias, F. Anğay, R. Mareus, C. Mastail, Texture and stress evolution in HfN films sputter-deposited at oblique angles, Coatings. 9 (2019) 712. doi:10.3390/coatings9110712.

[55] W. Phae-ngam, M. Horprathum, C. Chananonnawathorn, T. Lertvanithphol, B. Samransuksamer, P. Songsiriritthigul, H. Nakajima, S. Chaiyakun, Oblique angle deposition of nanocolumnar TiZrN films via reactive magnetron co-sputtering technique: The influence of the Zr target powers, Curr. Appl. Phys. 19 (2019) 894–901. doi:10.1016/j.cap.2019.05.002.

[56] M.J.M. Jimenez, V.G. Antunes, L.F. Zagonel, C.A. Figueroa, D. Wisnivesky, F. Alvarez, Effect of the period of the substrate oscillation in the dynamic glancing angle deposition technique: A columnar periodic nanostructure formation, Surf. Coatings Technol. 383 (2020) 125237. doi:10.1016/j.surfcoat.2019.125237.

[57] R. Alvarez, L. González-García, P. Romero-Gómez, V. Rico, J. Cotrino, A.R. Gonzlez-Elipe, A. Palmero, Theoretical and experimental characterization of TiO2 thin films deposited at oblique angles, J. Phys. D. Appl. Phys. 44 (2011) 385302. doi:10.1088/0022-3727/44/38/385302.

[58] K. Van Aeken, S. Mahieu, D. Depla, The metal flux from a rotating cylindrical magnetron: a Monte Carlo simulation, J. Phys. D. Appl. Phys. 41 (2008) 205307.

[59] J.F. Ziegler, J.P. Biersack, U. Littmark, The Stopping and Range of Ions in Matter, Pergamon Press, New York, 1985.

[60] D. Gall, S. Kodambaka, M.A. Wall, I. Petrov, J.E. Greene, Pathways of atomistic processes on TiN(001) and (111) surfaces during film growth: An ab initio study, J. Appl. Phys. 93 (2003) 9086–9094. doi:10.1063/1.1567797.

[61] Y. Ren, X. Liu, X. Tan, E. Westkämper, Adsorption and pathways of single atomistic processes on TiN (1 1 1) surfaces: A first principle study, Comput. Mater. Sci. 77 (2013) 102–107. doi:10.1016/j.commatsci.2013.04.036.

[62] C. Tholander, B. Alling, F. Tasnádi, J.E. Greene, L. Hultman, Effect of Al substitution on Ti, Al, and N adatom dynamics on TiN(001), (011), and (111) surfaces, Surf. Sci. 630 (2014) 28–40. doi:10.1016/j.susc.2014.06.010.

[63] R. Alvarez, J.M. Garcia-Martin, A. Garcia-Valenzuela, M. Macias-Montero, F.J. Ferrer, J. Santiso, V. Rico, J. Cotrino, A.R. Gonzalez-Elipe, A. Palmero, Nanostructured Ti thin films by magnetron sputtering at oblique angles, J. Phys. D. Appl. Phys. 49 (2016) 45303. doi:10.1088/0022-3727/49/4/045303.

[64] A. Stukowski, Visualization and analysis of atomistic simulation data with OVITO-the Open Visualization Tool, Model. Simul. Mater. Sci. Eng. 18 (2010) 15012. doi:10.1088/0965-0393/18/1/015012.

[65] J. Li, AtomEye: an efficient atomistic configuration viewer, Model. Simul. Mater. Sci. Eng. 11 (2003) 173–177.

[66] Y.G. Yang, D.D. Mass, H.N.G. Wadley, Porosity control in zig-zag vapor-deposited films, Thin Solid Films. 471 (2005) 1–11. doi:10.1016/j.tsf.2004.02.034.

[67] A.G. Dirks, H.J. Leamy, Columnar microstructure in vapor-deposited thin films, Thin Solid Films. 47 (1977) 219–233.

[68] H. Liang, X. Geng, W. Li, A. Panepinto, D. Thiry, M. Chen, R. Snyders, Experimental and modeling study of the fabrication of Mg nano-sculpted films by magnetron sputtering combined with glancing angle deposition, Coatings. 9 (2019) 361. doi:10.3390/coatings9060353.

[69] A. Chargui, R. El Beainou, A. Mosset, S. Euphrasie, V. Potin, P. Vairac, N. Martin, Influence of thickness and sputtering pressure on electrical resistivity and elastic wave propagation in oriented columnar tungsten thin films, Nanomaterials. 10 (2020) 81. doi:10.3390/nano10010081.

[70] A. Besnard, N. Martin, L. Carpentier, B. Gallas, A theoretical model for the electrical properties of chromium thin films sputter deposited at oblique incidence, J. Phys. D. Appl. Phys. 44 (2011) 215301. doi:10.1088/0022-3727/44/21/215301.

[71] R. Alvarez, A. Garcia-Valenzuela, V. Rico, J.M. Garcia-Martin, J. Cotrino, A.R. Gonzalez-Elipe, A. Palmero, Kinetic energy-induced growth regimes of nanocolumnar Ti thin films deposited by evaporation and magnetron sputtering, Nanotechnology. 30 (2019) 475603.

[72] P. Patsalas, C. Gravalidis, S. Logothetidis, Surface kinetics and subplantation phenomena affecting the texture, morphology, stress, and growth evolution of titanium nitride films, J. Appl. Phys. 96 (2004) 6234–6235. doi:10.1063/1.1811389.

[73] J.A. Thornton, The microstructure of sputter-deposited coatings, J. Vac. Sci. Technol. A Vacuum, Surfaces, Film. 4 (1986) 3059–3065. doi:10.1116/1.573628.

[74] S. Mahieu, P. Ghekiere, D. Depla, R. De Gryse, Biaxial alignment in sputter deposited thin films, Thin Solid Films. 515 (2006) 1229–1249. doi:10.1016/j.tsf.2006.06.027.

[75] S. Mukherjee, D. Gall, Structure zone model for extreme shadowing conditions, Thin Solid Films. 527 (2013) 158–163. doi:10.1016/j.tsf.2012.11.007.

[76] A. Panepinto, R. Snyders, Recent advances in the development of nano-sculpted films by magnetron sputtering for energy-related applications, Nanomaterials. 10 (2020) 2039. doi:10.3390/nano10102039.

[77] C. Lopez-Santos, R. Alvarez, A. Garcia-Valenzuela, V. Rico, M. Loeffler, A.R. Gonzalez-Elipe, A. Palmero, Nanocolumnar association and domain formation in porous thin films grown by evaporation at oblique angles, Nanotechnology. 27 (2016) 395702. doi:10.1088/0957-4484/27/39/395702.

[78] D. Vick, T. Smy, M.J. Brett, Growth behavior of evaporated porous thin films, J. Mater. Res. 17 (2002) 2904–2911. doi:10.1557/JMR.2002.0421.

[79] J. Colin, A. Jamnig, C. Furgeaud, A. Michel, N. Pliatsikas, K. Sarakinos, G. Abadias, In situ and real-time nanoscale monitoring of ultra-thin metal film growth using optical and electrical diagnostic tools, Nanomaterials. 10 (2020) 2225. doi:10.3390/nano10112225.

[80] R. Mareus, C. Mastail, F. Anğay, N. Brunetière, G. Abadias, Study of columnar growth, texture development and wettability of reactively sputter-deposited TiN, ZrN and HfN thin films at glancing angle incidence, Surf. Coatings Technol. 399 (2020) 126130. doi:10.1016/j.surfcoat.2020.126130.

[81] H. Badorreck, M. Steinecke, L. Jensen, D. Ristau, M. Jupé, J. Müller, R. Tonneau, P. Moskovkin, S. Lucas, A. Pflug, L. Grinevičiūtė, A. Selskis, T. Tolenis, Correlation of structural and optical properties using virtual materials analysis, Opt. Express. 27 (2019) 22209. doi:10.1364/oe.27.022209.

MODENA kMC code

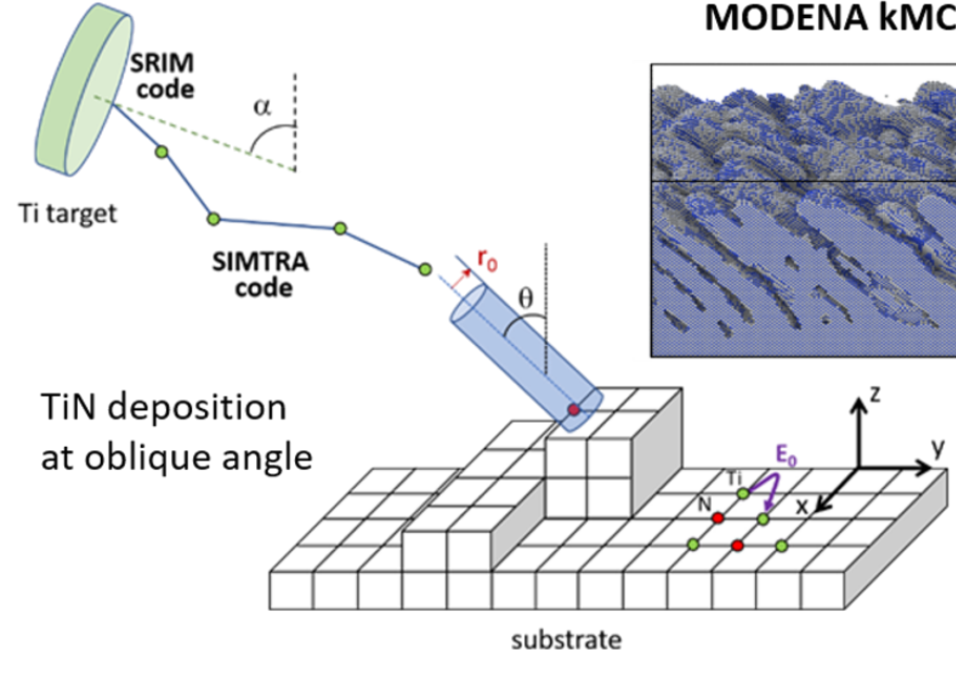

Influence of temperature